

Field-induced abrupt change in magnetization of the manganite compounds (LaR)_{0.45}(CaSr)_{0.55}MnO₃ (R=Eu and Tb)

D. S. Rana,^{1,*} D. G. Kuberkar,² and S. K. Malik^{1,†}¹Tata Institute of Fundamental Research, Colaba, Mumbai-400 005, India²Department of Physics, Saurashtra University, Rajkot-360 005, India

(Received 26 September 2005; published 6 February 2006)

The ABO₃ type manganites (LaR)_{0.45}(CaSr)_{0.55}MnO₃ (R=Eu³⁺—a nonmagnetic ion and Tb³⁺—a magnetic ion) which possess large A-site size-disorder, exhibit metamagnetic transitions as a function of magnetic field. Below a certain crossover temperature and depending on the magnetic field sweep rate, the metamagnetic transition transforms from a broad to sharp step-like transitions. This crossover temperature increases on increasing the field sweep rate. The effect of field sweep rate on the critical field of metamagnetic steps decreases with decreasing temperature. This along with the magnetic relaxation and specific heat data provide clear evidence on the contribution of spin-lattice coupling in determining the transformation from smooth to sharp magnetic transitions. These studies also suggest that the A-site magnetism has no important role in transformation from reversible to irreversible magnetization.

DOI: 10.1103/PhysRevB.73.064407

PACS number(s): 75.47.Gk, 75.47.Lx

During the past decade, the ABO₃ perovskite type mixed-valent manganites of the general formula R_{1-x}A_xMnO₃ (R=trivalent rare-earth ion and A=divalent cation) have been widely investigated. These compounds are interesting owing to their correlated structural, transport, and magnetic properties coupled with a large magnetoresistance effect in the hole-doped regime (i.e., $x < 0.5$) (for a review, see Refs. 1 and 2). An interesting evolution of different magnetic ground states takes place in these compounds as x varies from 0 to 1. In hole-doped manganites ($x < 0.5$), the ferromagnetic (FM) metallic state dominates as a result of Zener-Double Exchange interactions. At the periphery of half-doping ($x = 0.5$); various spin, charge, and orbital orderings induce antiferromagnetic (AFM) state, which become more robust in the largely divalent cation-doped region (when $x > 0.5$).¹⁻³ At half-doping, the charge-ordered and AFM state in certain compositions, like La_{0.5}Ca_{0.5}MnO₃, Pr_{0.5}Sr_{0.5}MnO₃, etc., is susceptible to external factors such as temperature, magnetic field, pressure, etc.³⁻⁹ Further, when x varies between 0.5 and 1, different kinds of AFM spin arrangements manifest. As x increases in this region, the A-type of layered AFM spin arrangement and orbital ordered states appear which are not susceptible to moderate external factors.²

The temperature and magnetic field induced magnetic phase transitions in manganites also depend upon factors such as: (i) A geometrical index called the tolerance factor (defined as $t = \{(r_A) + r_O\} / \sqrt{2\{(r_B) + r_O\}}$), (ii) the size-disorder at the A-site (quantified as $\sigma^2 = \sum x_i r_i^2 - \langle r_A \rangle^2$), and (iii) the impurity doping at the Mn-site.^{1-3,10} Some Pr-based half-doped and hole-doped compounds possess a smaller tolerance factor and, therefore, their charge and orbital ordered (CO and OO) AFM state^{7-9,11-16} is rather stable as compared to those of having a larger tolerance factor. The study of magnetic field induced phase transitions in such CO and OO Pr-based systems has recently become the focus of research in manganites because of the following special features.¹¹⁻¹⁶ These compounds exhibit sharp step-like metamagnetic transitions at low temperatures. The critical field of these metamagnetic

transitions varies as a function of chemical substitution, temperature, field, and time. These transitions are primarily a result of phase separation, which is induced either by diluting the Mn sub-lattice or by creating a large size-disorder at the A-site. However, these fascinating metamagnetic properties have been observed mostly in Pr-based hole-doped and half-doped compounds only,¹¹⁻¹⁶ with some of the properties such as irreversibility of magnetization isotherms attributed to the ordering of Pr magnetic moments.¹⁶ Apart from hole-doped and half-doped compounds, such metamagnetic steps have not been studied thoroughly in compounds having divalent cation content $\geq 50\%$. More importantly, the transformation from a smooth to a step-like AFM to FM transition at low temperatures ($T \leq 5$ K) also prompted us to investigate the structural (lattice) contribution in behavioral change in such first-order phase transitions.

In this article, we report the results of magnetization studies in the 55% divalent cation doped compounds (La_{0.2}Eu_{0.25})(Ca_{0.3}Sr_{0.25})MnO₃ (to be referred to as 'LE-55') and (La_{0.325}Tb_{0.125})(Ca_{0.3}Sr_{0.25})MnO₃ (LT-55). The divalent cation content (55%) in these compounds is near the half-doping level. Therefore, an AFM spin arrangement is the most probable magnetic state. These compounds exhibit metamagnetic transitions as a function of magnetic field. The multiple cation substitution at the A-site with a nonmagnetic rare-earth ion, Eu³⁺, and a magnetic rare-earth ion, Tb³⁺, has been made because of the following reasons: (i) The size-disorder at the A-site is large, which is likely to induce phase separation, (ii) the simultaneously substitution of rare earth ion (Eu³⁺ or Tb³⁺) and Sr²⁺ keeps the average A-site cation radius ($\langle r_A \rangle$) of both the samples nearly same [see Table I], (iii) the nonmagnetic and the magnetic nature of Eu³⁺ and Tb³⁺ ions, respectively, will help us elucidate the contribution of A-site magnetism, if any, on the metamagnetic properties. The A-site disorder induces phase separation, which causes field-induced and temperature-dependent, smooth and sharp step-like AFM to FM first-order phase transitions. In this study, we establish from magnetization,

TABLE I. Unit cell parameters (a)–(c), average A-site cation radius ($\langle r_A \rangle$) and A-site size-disorder (σ^2) for $(\text{La}_{0.2}\text{Eu}_{0.25}) \times (\text{Ca}_{0.3}\text{Sr}_{0.25})\text{MnO}_3$ (LE-55) and $(\text{La}_{0.325}\text{Tb}_{0.125}) \times (\text{Ca}_{0.3}\text{Sr}_{0.25})\text{MnO}_3$ (LT-55) samples (structure: orthorhombic, space group: $Pnma$, No. 62).

Samples	a (Å)	b (Å)	c (Å)	$\langle r_A \rangle$ (Å)	σ^2 (Å ²)
LE-55	5.426(1)	7.644(1)	5.423(1)	1.205	~ 0.005
LT-55	5.426(4)	7.648(2)	5.434(3)	1.213	~ 0.004

magnetic relaxation and calorimetric investigations that, at low temperatures, the depleting lattice energy and, hence, the weak spin-lattice coupling results in sharp magnetic transitions.

The $(\text{La}_{0.2}\text{Eu}_{0.25})(\text{Ca}_{0.3}\text{Sr}_{0.25})\text{MnO}_3$ (LE-55) and $(\text{La}_{0.325}\text{Tb}_{0.125})(\text{Ca}_{0.3}\text{Sr}_{0.25})\text{MnO}_3$ (LT-55) samples were synthesized using the standard solid-state reaction method. Constituent oxides (La_2O_3 , Eu_2O_3 , Tb_2O_3 and MnO_2) and carbonates (SrCO_3 and CaCO_3) were mixed thoroughly in stoichiometric proportions and calcined at 950 °C for 24 h. These were ground, pelletized, and sintered in the temperature range of 1100 °C–1250 °C for 100 h with many intermediate grindings. The final sintering was carried out at 1350 °C for 24 h. X-ray diffraction (XRD) patterns were recorded in the 2θ range of 20°–80° on a Siemens diffractometer. Magnetization and a.c. susceptibility measurements were performed using a SQUID magnetometer (MPMS XL, Quantum Design) and PPMS (Quantum Design). While collecting data for the isothermal magnetizations, the samples were warmed to 250 K (well above any magnetic ordering temperature) to remove any magnetic history effects. The magnetic relaxation (magnetization vs time) measurements at various temperatures were performed after cooling the sample in a field of 70 kOe. The sample was warmed every time up to 250 K for successive relaxation measurements at different temperatures. The XRD patterns showed that LE-55 and LT-55 samples are single-phase compounds crystallizing in a distorted orthorhombic structure (space group $Pnma$, No. 62). Rietveld refinement of the XRD data of these samples (using the computer code FULLPROF) showed an excellent agreement with experimental patterns. The refined cell parameters are given in Table I and agree well with the trend of their $\langle r_A \rangle$ values and hence, their tolerance factors.

Figure 1 shows the magnetization of $(\text{La}_{0.2}\text{Eu}_{0.25}) \times (\text{Ca}_{0.3}\text{Sr}_{0.25})\text{MnO}_3$ and $(\text{La}_{0.325}\text{Tb}_{0.125})(\text{Ca}_{0.3}\text{Sr}_{0.25})\text{MnO}_3$ samples as a function of magnetic field (field sweep rate of 200 Oe/sec) at 2, 3, 5, and 10 K. Both samples exhibit metamagnetic transitions in the vicinity of a field of 70 kOe in all the M-H isotherms shown in Fig. 1. At 5 and 10 K, the magnetic transitions are broad with a width spanning a magnetic field of ~ 20 kOe, while at 3 and 2 K, these transition are sharp, step-like with a transition width of only 0.5 kOe. At 2 K, the (critical field) H_C for the first magnetic step is ~ 72 kOe for LE-55 sample and ~ 63 kOe for LT-55 sample. The spontaneous magnetization attains a value of $\sim 1.8 \mu_B$ for LE-55 and $\sim 2.5 \mu_B$ for LT-55 sample in a field of 90 kOe vis-a-vis theoretically calculated saturation magnetization (M_S) of $\sim 3.45 \mu_B$.¹⁷ The difference between the

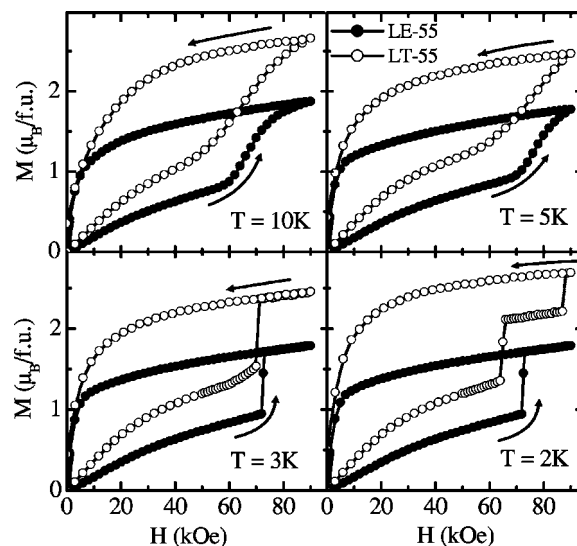


FIG. 1. Magnetization (M) vs field (H) isotherms at 10, 5, 3, and 2 K for $(\text{La}_{0.2}\text{Eu}_{0.25})(\text{Ca}_{0.3}\text{Sr}_{0.25})\text{MnO}_3$ (LE-55) and $(\text{La}_{0.325}\text{Tb}_{0.125})(\text{Ca}_{0.3}\text{Sr}_{0.25})\text{MnO}_3$ (LT-55) samples.

spontaneous magnetization and M_S for these samples reveals that AFM state is not completely transformed to FM state. This is attributed to the fact that 55% divalent cation doped compounds possess a robust AFM state. For instance, in a similar divalent cation doped compound, $\text{Nd}_{0.45}\text{Sr}_{0.55}\text{MnO}_3$, the AFM state is highly stable and the H_C required for transition from AFM to FM state is greater than 300 kOe.⁸ In LE-55 and LT-55 samples, the large size-disorder at the A-site, most likely, results in phase separated FM and AFM states. Though, an applied field of 90 kOe induces large FM phase in these samples, it is not sufficient to transform the AFM state completely to a FM state. Analogous to the metamagnetic transition, field induced transitions occur in specific heat isotherms for LE-55 sample at 5 and 2 K. These data are shown in Fig. 2, from which it is clearly seen that the transition is dominant at 5 K but weak at 2 K. Both in the magnetization and specific heat data, though the transitions occur at nearly the same H_C , the trend of irreversibility in these transitions displays inverse relation, which will be discussed later.

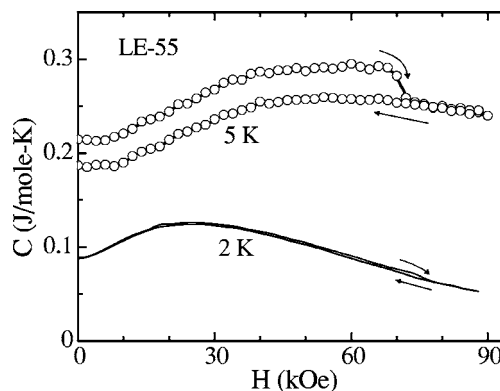


FIG. 2. Specific heat (C) vs field (H) isotherms at 5 and 2 K for $(\text{La}_{0.2}\text{Eu}_{0.25})(\text{Ca}_{0.3}\text{Sr}_{0.25})\text{MnO}_3$ (LE-55) sample.

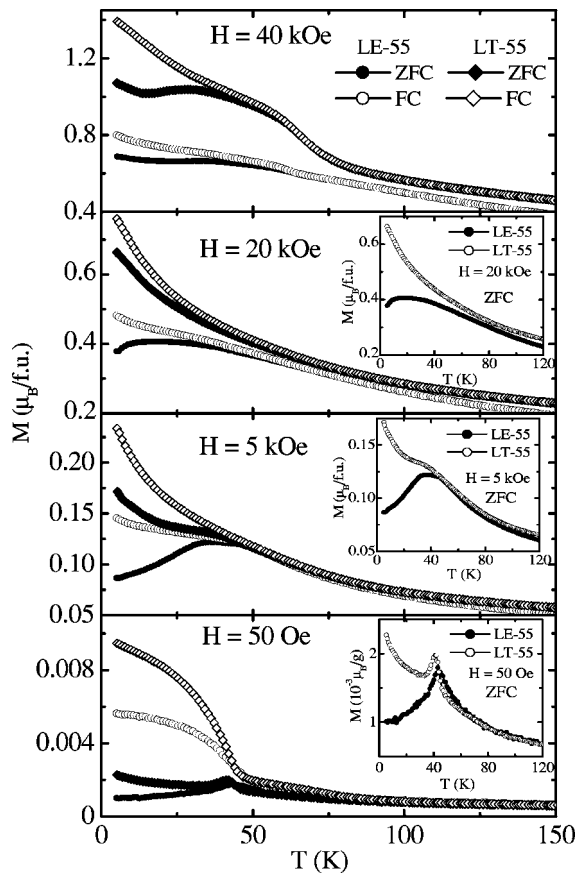


FIG. 3. Zero-field-cooled (ZFC) and field-cooled (FC) magnetization (M) vs temperature (T) in fields of 50 Oe, 5 kOe, 20 kOe, and 40 kOe for $(\text{La}_{0.2}\text{Eu}_{0.25})(\text{Ca}_{0.3}\text{Sr}_{0.25})\text{MnO}_3$ (LE-55) and $(\text{La}_{0.325}\text{Tb}_{0.125})(\text{Ca}_{0.3}\text{Sr}_{0.25})\text{MnO}_3$ (LT-55) samples. Insets in the three panels show the ZFC magnetization in the respective fields for the same samples.

The phase separation may be studied from the temperature dependence of magnetization. Figure 3(a) shows the plot of zero-field-cooled (ZFC) and field-cooled (FC) magnetization (M) of $(\text{La}_{0.2}\text{Eu}_{0.25})(\text{Ca}_{0.3}\text{Sr}_{0.25})\text{MnO}_3$ and $(\text{La}_{0.325}\text{Tb}_{0.125})(\text{Ca}_{0.3}\text{Sr}_{0.25})\text{MnO}_3$ samples as a function of temperature between 5 and 150 K in fields of 50 Oe, 5 kOe, 20 kOe, and 40 kOe. Both the samples exhibit a peak in M_{ZFC} nearly at the same temperature (~ 46 K in a field of 50 Oe). This is followed by a large bifurcation of M_{ZFC} and M_{FC} curves below this peak, which is reminiscent of cluster spin-glass behavior. Such a behavior is a signature of competing FM and AFM phase interactions and, hence, points towards the phase separation. Recently similar cluster-glass behavior has been reported in other phase-separated manganite systems.¹⁸ It is seen that the M_{ZFC} of the two samples is qualitatively similar above 46 K peak. However, below this peak temperature, the M_{ZFC} decreases for LE-55 sample whereas it increases at about 30 K for LT-55 sample. This rise in M_{ZFC} of LT-55 sample is moderate in 50 Oe but becomes dominant at higher fields of 5 and 20 kOe to the extent that it suppresses the peak. On the other hand, the M_{ZFC} of LE-55 sample decreases below the peak in fields of 50 Oe, 5 kOe, and 20 kOe. This remarkable difference in

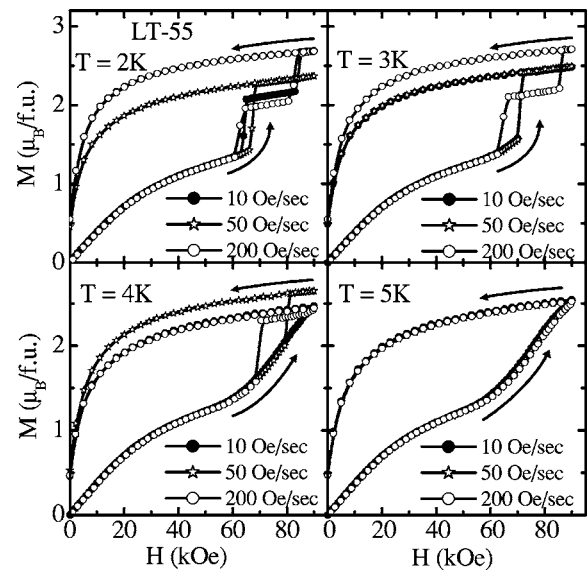


FIG. 4. Magnetization (M) vs field (H) isotherms at 2, 3, 4, and 5 K in magnetic field sweep rates of 10, 50, and 200 Oe/s for $(\text{La}_{0.325}\text{Tb}_{0.125})(\text{Ca}_{0.3}\text{Sr}_{0.25})\text{MnO}_3$ (LT-55) sample.

M_{ZFC} of the two samples below 46 K is attributed to the paramagnetic contribution of Tb^{3+} ions in LT-55 sample. Another evidence of this paramagnetic contribution is the quasi-linear dependence of magnetization on field as seen from the magnetic isotherms in Fig. 1. Hence, these two observations make it clear that the Tb^{3+} ions do not exhibit any magnetic ordering and rather remain paramagnetic down to low temperatures. Another discernible feature that evolves in magnetization of LT-55 sample in 40 kOe is its enhanced magnetization as compared to that of LE-55 sample in the temperature range of 70–20 K. Since this sample has $H_{\text{C}} \sim 60$ kOe, the larger magnetization in 40 kOe may have its origin in field induced onset of transformation of an AFM to a FM state.

The fascinating feature of the present studies on $(\text{La}_{0.2}\text{Eu}_{0.25})(\text{Ca}_{0.3}\text{Sr}_{0.25})\text{MnO}_3$ and $(\text{La}_{0.325}\text{Tb}_{0.125})(\text{Ca}_{0.3}\text{Sr}_{0.25})\text{MnO}_3$ samples is the observation of sharp step-like metamagnetic transitions. *Observation of these steps in the present compounds having divalent cation >50% makes these systems unique since earlier such steps were mostly seen in compounds with divalent cation content of $\leq 50\%$.* In order to understand the transformation from broad metamagnetic transitions to sharp ones as a function of varying temperature and field sweep rate of magnetic field, the magnetization isotherms for LE-55 and LT-55 samples were recorded with magnetic field sweep rates of 10, 50, and 200 Oe/s at temperatures of 2, 3, 4, and 5 K (Fig. 4). It is observed that, on varying the field sweep rate, the critical field (H_{C}) of the metamagnetic transition changes (Table II) and this variation of H_{C} is temperature dependent. For instance, at 2 K, the overall variation of H_{C} with magnetic field sweep rate is small at 2 K. At 3 K, the isotherms obtained at sweep rate of 10 and 50 Oe/s exhibit similar H_{C} of ~ 70 kOe which decreases to ~ 62 kOe as the sweep rate is enhanced to 200 Oe. Further, the metamagnetic transition displays a fascinating behavior at 4 K; the isotherm recorded

TABLE II. Critical magnetic field (H_C) of metamagnetic transition at magnetic field sweep rates of 10, 50, and 200 Oe/s for $(La_{0.325}Tb_{0.125})(Ca_{0.3}Sr_{0.25})MnO_3$.

Temperature (K)	Critical magnetic field (H_C) Magnetic field sweep rate		
	10 Oe/s (kOe)	50 Oe/s (kOe)	200 Oe/s (kOe)
2	62	66	60
3	70	70	62
4	No step	80	69

at 10 Oe/s sweep rate shows a broad transition whereas that recorded at 50 Oe/s sweep rate shows a sharp transition with $H_C \sim 80$ kOe, which decreases considerably to ~ 69 kOe in field sweep rate of 200 Oe/s. At 5 K, all metamagnetic transitions are broad and similar in all the field sweep rates. These observations help us to derive important information about the sweep rate dependence of H_C at different temperatures and disappearance of steps. It has been reported that in phase-separated Pr-based manganites, the broad metamagnetic transition transforms to sharp step-like transitions below a certain temperature (called crossover temperature). However, as is evident from the present studies on LT-55 sample, at 4 K, the metamagnetic transitions are sharp but smear to a broader transition at low-field sweep rate. *This shows that the crossover temperature also depends on the magnetic field sweep rate and shifts to higher values with increasing field sweep rate.* Another noteworthy feature is that, at 2 K, the dependence of H_C on sweep rate is small (Table II) and it increases at 3 K. However, as the temperature is raised in the vicinity of the crossover temperature (e.g., 4 K), the effect of field sweep rate appears to an extent that broad metamagnetic transition at low field sweep rate (10 kOe/s) sharpens on increasing the sweep rate to 50 Oe/s and H_C decreases considerably with further increasing the field sweep rate. *This implies that the H_C near the crossover point decreases considerably with increase in field sweep rate and as temperature is further decreased the effect of sweep rate on H_C decreases.*

In all above-mentioned metamagnetic transitions in low temperature region ($T \leq 10$ K), it is seen that the magnetic isotherms irreversible. Here, the irreversibility implies that the FM state, which appears after the metamagnetic transition, does not return to the initial AFM state after the magnetic field is removed. To study the effect of increasing temperature on this irreversibility and the shape of isotherm when magnetization is measured in five quadrants of positive and negative field, the magnetic isotherms for LE-55 and LT-55 samples were recorded as $0 \text{ Oe} \rightarrow +90 \text{ kOe} \rightarrow -90 \text{ kOe} \rightarrow +90 \text{ kOe} \rightarrow 0 \text{ Oe}$ at 2, 20, and 50 K and are shown in Fig. 5. At any fixed temperature, the isotherms of both the samples are qualitatively similar. For instance, at 50 K, the isothermal magnetization curves of these compounds display reversible and symmetric behavior (i.e., magnetization obtained while scanning the field as $0 \text{ Oe} \rightarrow +90 \text{ kOe} \rightarrow 0 \text{ Oe}$ is symmetric with that obtained from subsequent field scan

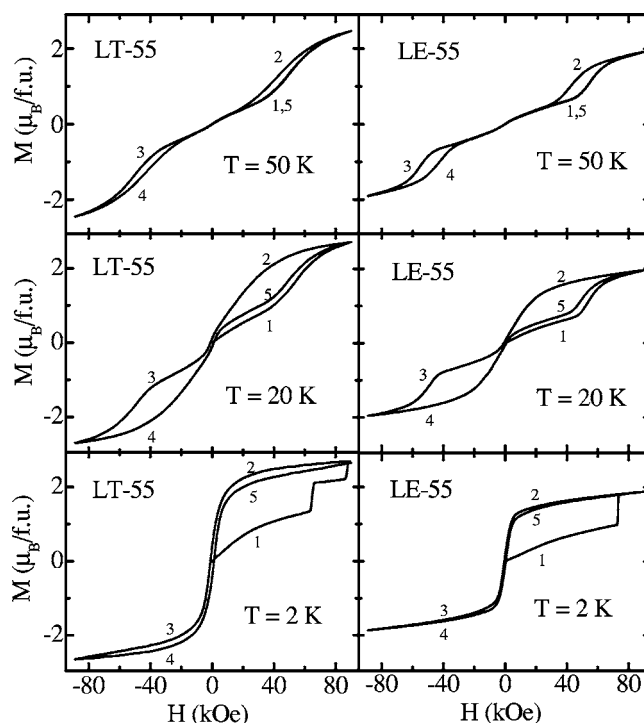


FIG. 5. Five-quadrant magnetization (M) vs field (H) isotherms at 50, 20, and 2 K for $(La_{0.2}Eu_{0.25})(Ca_{0.3}Sr_{0.25})MnO_3$ (LE-55) and $(La_{0.325}Tb_{0.125})(Ca_{0.3}Sr_{0.25})MnO_3$ (LT-55) samples. The field was scanned as $0 \text{ T} \rightarrow (+9 \text{ T}) \rightarrow 0 \text{ T} \rightarrow (-9 \text{ T}) \rightarrow 0 \text{ T} \rightarrow (+9 \text{ T})$ with $0 \text{ T} \rightarrow (+9 \text{ T})$ coded as “1” followed by every subsequent field scans coded as 2–5.

as $0 \text{ Oe} \rightarrow -90 \text{ kOe} \rightarrow 0 \text{ Oe}$). However, the isotherm at 20 K exhibits irreversible and asymmetric behavior and the irreversibility gets rather dominant at 2 K. With decreasing temperature, such a transformation from reversible to irreversible isothermal magnetization, both in LE-55 and LT-55, is similar to that reported in Pr-based manganites. In Pr-based compounds, where Pr moments are known to order magnetically, the irreversibility is thought to be induced by pinning of Mn-moments in FM state by the ordered Pr magnetic moments.¹⁶ In contrast to the situation in Pr-based compounds; there is no evidence for the ordering of magnetic moments of A-site cations in LE-55 and LT-55 samples. This suggests that the origin of irreversible isothermal magnetization along with the occurrence of sharp steps in Pr-based manganites and in the LE-55 and LT-55 samples appears to be a rather more general effect. Further, this effect does not seem to be related to the magnetic character of A-site cations but may arise from the temperature dependent spin-phonon coupling, as discussed below.

As seen in Figs. 1 and 4, there exists a crossover temperature ($T \sim 4$ K), at which broad and smooth metamagnetic transitions apparently become sharp step-like transitions. The sharpness of these metamagnetic transitions and their dependence on the temperature and the magnetic field sweep rate may be explained by invoking the phase-separation scenario and the temperature dependent spin-phonon coupling. In phase-separated state, the FM and AFM phases are associated with different crystallographic structures, which has

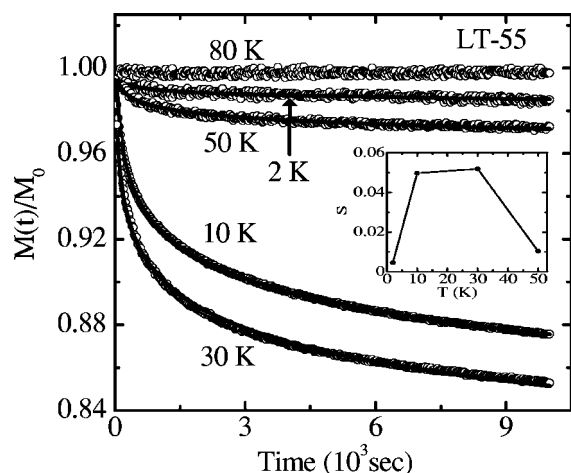


FIG. 6. Magnetic relaxation (normalized magnetization vs time) plots for $(\text{La}_{0.325}\text{Tb}_{0.125})(\text{Ca}_{0.3}\text{Sr}_{0.25})\text{MnO}_3$ (LT-55) sample. The data was collected after cooling the sample in a field of 70 kOe and then reducing the field to zero. To measure the magnetic relaxation at each temperature, the sample was heated every time up to a temperature of 250 K and then cooled in field of 70 kOe. The symbols are the experimental data while the continuous lines are fits to the logarithmic decay law (except at 80 K). Inset in the figure shows the magnetic viscosity (S) as a function of temperature (T).

been evidenced by neutron diffraction studies recently.²⁰ This observation along with the role of lattice energy (or phonons) becomes important in understanding the transformation from a smooth to step-like transitions at low temperatures. Magnetic relaxation and specific heat data provide us clear evidence and better understanding on the role of spin-lattice (phonon) coupling on the temperature dependent qualitative aspects of metamagnetic transitions. Figure 6 shows the plot of normalized magnetization ($M(t)/M_0$) vs time (t) for LT-55 sample at various temperatures when the sample was cooled in a field of 70 kOe to a specific temperature at which relaxation was measured. In a field of 70 kOe, a considerable fraction of AFM phase transforms to FM phase and, therefore, it is most appropriate field regime to probe the contribution of lattice during the kinetics of AFM to FM transitions. Except at 80 K, the magnetic relaxation at all other temperatures obeys logarithmic decay law which characteristics of glassy systems and is given by $M(t) = M_0(1 - S \log_{10}(t/\tau))$, where S (magnetic viscosity) is a constant that denotes the relaxation rate.²¹ It is clear from Fig. 6 that there is no magnetic relaxation at 80 K, which is well above the glassy transition temperature (~ 46 K, Fig. 3), while there is only a weak relaxation at 50 K. However, the values of S (inset in Fig. 6) depict that the relaxation is considerably large at 30 and 10 K but it nearly diminishes at 2 K. Here, a significant difference in relaxation rates at close temperatures of 10 and 2 K is likely to arise from difference in the lattice-spin coupling at these respective temperatures. The diminishing lattice energy is also evident from isothermal specific heat vs magnetic field data measured at 5 and 2 K for LE-55 sample (Fig. 2). While a broad irreversible drop in specific heat occurs in 5 K isotherm, there is no discernible irreversibility in the 2 K isotherm. On the other hand, there is an enhancement in irreversibility in magnetic isotherms as tem-

perature is decreased (Fig. 1). The specific heat (C_p) arises from major contributions of the conduction electrons and the lattice ($C_p = \gamma T + \beta T^3$). These samples are insulators and it is known that there is almost no electronic contribution (γT) at low temperatures. It is the lattice contribution (βT^3) that decreases largely at low temperatures. At 5 K (i.e., region of smooth metamagnetic transitions), the lattice contribution and, hence, the spin-lattice coupling is sufficient to exhibit a transition in specific heat while, at 2 K (i.e., region of sharp metamagnetic steps), due to lower lattice contribution, the irreversible transition almost disappears. These aspects have direct relations with the relaxation data (Fig. 6) in which significantly large relaxation at 10 K implies that the spins tend to relax through the lattice when the latter has sufficient energy. A sudden disappearance of relaxation at 2 K further shows that spins do not find sufficient energy in the lattice to relax.

The above-mentioned experimental evidences of rapid reduction in the lattice energy and poor spin-lattice coupling at low temperatures, explain the mechanism of transformation from broad to sharp magnetic transitions as follows. In temperature regime of smooth transitions, the spins are firmly coupled to the lattice during the kinetics of AFM to FM phase transitions. This causes a smooth and unhindered growth of FM spin moments through lattice resulting in smooth transitions. However, as the temperature is lowered to the regime of weak spin-lattice coupling, the systems tends to deplete the energy at the FM and AFM structural interfaces. Now, the applied magnetic field generates strain at these interfaces and, therefore, during the kinetics of phase transition, a smooth growth of FM phase is inhibited. But at a certain critical magnetic field, the energy barrier is overcome resulting in a sudden step-like AFM to FM phase transition. This transformation takes place through multiple steps as the transition is arrested at an intermediate magnetic state due to insufficient energy gained from magnetic field. In such a state, it is obvious that the volume of FM phase fraction is large and, hence, a larger strain exists at the two structural interfaces. Now, the extra energy gained from further increasing the magnetic field overcomes this strain and results in the subsequent magnetic steps. The presence of strain in the presently studied samples (which may be random) is inferred from the magnetization isotherms at 2 K for LT-55 sample recorded three times consecutively (each time after warming the sample to 300 K). It is observed that the H_C , both of the first and the second step, in all the M-H isotherms, is not exactly the same (Fig. 7). For instance, the H_C of the first step has a variation of 1.5 kOe while that of the second step has a larger variation of 2.5 kOe. These different values of H_C under similar conditions indicate that the release of strain is random and is a cause of sharp step like transitions at $T \leq 4$ K.

The observation that the effect of magnetic field sweep rate on the critical field of magnetic steps is temperature dependent (Fig. 4), can also be explained in the light of depleted lattice energy at low temperatures as follows. In the vicinity of the crossover temperature (~ 4 K), the H_C is more dependent on the field sweep rate. Here, the increase in H_C of step and the disappearance of steps with decreasing field

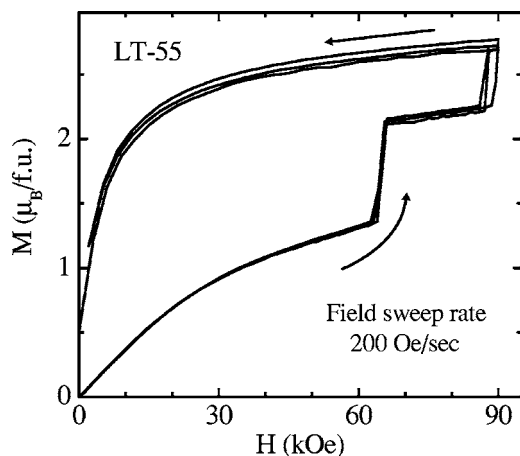


FIG. 7. Magnetization vs field isotherms at 2 K in magnetic field sweep rate of 200 Oe/s for $(\text{La}_{0.325}\text{Tb}_{0.125})(\text{Ca}_{0.3}\text{Sr}_{0.25})\text{MnO}_3$ (LT-55) sample recorded three times consecutively.

sweep rate is associated with the accumulation and the subsequent release of strains with time, or in other words, spin gaining energy from lattice with time. This is because a sweep rate of 10 Oe/s takes substantially longer time to record an M-H isotherm. During this time the spins may gain energy from the lattice in a cumulative way and the catastrophe of steps is delayed or prohibited. However, at lower

temperature of 2 K (Fig. 4), a weak dependence of H_C on field sweep rate suggests that due to the almost depleted lattice energy, spins do not get any energy from the lattice irrespective of the large time taken to sweep the field and, therefore, the step-like catastrophe is inevitable.

In summary, we have studied detailed magnetic properties of 55% divalent cation doped $(\text{La}_{0.2}\text{Eu}_{0.25}) \times (\text{Ca}_{0.3}\text{Sr}_{0.25})\text{MnO}_3$ and $(\text{La}_{0.325}\text{Tb}_{0.125})(\text{Ca}_{0.3}\text{Sr}_{0.25})\text{MnO}_3$ compounds. In both these A-site disordered samples, a magnetic field of around 70 kOe destabilizes the AFM state via metamagnetic transitions to FM state. The magnetic relaxation and calorimetric investigations establish that a low temperature crossover from smooth to sharp metamagnetic transitions originates from the reduced lattice energy and resulting weak spin-lattice coupling. We show that in the vicinity of crossover temperature, the critical field for step-like transitions decreases significantly with increase in field sweep rate, but as the temperature decreases, critical field is weakly affected by field sweep rate. The transformation from reversible to an irreversible magnetization in these samples is similar to that observed in Pr-based manganites in which Pr moments order magnetically. The present work suggests that the irreversible metamagnetic is a more general effect in which the temperature dependent spin-lattice coupling is responsible for this property while the magnetism of A-site cation may not be very important.

*Present address: Institute of Laser Engineering, Osaka University, 2-6 Yamadaoka, Suita, Osaka, Japan.

Email: rana-d@ile.osaka-u.ac.jp

†Corresponding author. Email: skm@tifr.res.in

¹*Colossal Magnetoresistance, charge ordering and other related properties of rare earth manganates*, edited by C. N. R. Rao and B. Raveau (World Scientific, Singapore, 1998).

²E. Dagotto, T. Hotta, and A. Moreo, *Phys. Rep.* **344**, 1 (2001).

³C. N. R. Rao and A. K. Cheetam, *Chem. Mater.* **10**, 2714 (1998), and references therein.

⁴Y. Tomioka, A. Asamitsu, Y. Moritomo, H. Kuwahara, and Y. Tokura, *Phys. Rev. Lett.* **74**, 5108 (1995).

⁵E. O. Wollan and W. C. Koehler, *Phys. Rev.* **100**, 545 (1955); P. G. Radaelli, D. E. Cox, M. Marezio, S. W. Cheong, P. E. Schiffer, and A. P. Ramirez, *Phys. Rev. Lett.* **75**, 4488 (1995).

⁶H. Kuwahara, Y. Moritomo, Y. Tomioka, A. Asamitsu, M. Kasai, R. Kumai, and Y. Tokura, *Phys. Rev. B* **56**, 9386 (1997).

⁷H. Kuwahara, Y. Tomoika, A. Asamitsu, Y. Moritomo, and Y. Tokura, *Science* **270**, 961 (1995).

⁸T. Hayashi, N. Miura, K. Noda, H. Kuwahara, S. Okamoto, S. Ishihara, and S. Maekawa, *Phys. Rev. B* **65**, 024408 (2001).

⁹M. Tokunaga, N. Miura, Y. Tomioka, and Y. Tokura, *Phys. Rev. B* **57**, 5259 (1998).

¹⁰L. M. Rodriguez-Martinez and J. P. Attfield, *Phys. Rev. B* **54**, 15622 (1996).

¹¹R. Mahendiran, A. Maignan, S. Hebert, C. Martin, M. Hervieu, B. Raveau, J. F. Mitchell, and P. Schiffer, *Phys. Rev. Lett.* **89**,

286602 (2002).

¹²V. Hardy, A. Maignan, S. Hebert, and C. Martin, *Phys. Rev. B* **67**, 024401 (2003).

¹³T. Wu and J. F. Mitchell, *Phys. Rev. B* **69**, 100405(R) (2004).

¹⁴V. Hardy, S. Majumdar, S. J. Crowe, M. R. Lees, D. McK. Paul, L. Herve, A. Maignan, S. Hebert, C. Martin, C. Yaicle, M. Hervieu, and B. Raveau, *Phys. Rev. B* **69**, 020407(R) (2004), and references therein.

¹⁵L. Ghivelder, R. S. Freitas, M. G. das Virgens, H. Martinho, L. Granja, G. Leyva, P. Levy, and F. Parisi, *Phys. Rev. B* **69**, 214414 (2004).

¹⁶Joonghoe Dho and N. H. Hur, *Phys. Rev. B* **67**, 214414 (2003).

¹⁷ M_S is calculated from the spin only values of Mn ions using the relation, $M_S = gS\mu_B$ and is $\sim 3.45 \mu_B$ for the compounds with 55% divalent cation content. Also, it may be mentioned here that in manganites, the Tb^{3+} does not order ferromagnetically down to 2 K and only its paramagnetic moments add to the total magnetic moment.

¹⁸F. Rivadulla, M. A. Lopez-Quintela, and J. Rivas, *Phys. Rev. Lett.* **93**, 167206 (2004).

¹⁹D. E. Cox, P. G. Radaelli, M. Marezio, and S.-W. Cheong, *Phys. Rev. B* **57**, 3305 (1998).

²⁰F. M. Woodward, J. W. Lynn, M. B. Stone, R. Mahendiran, P. Schiffer, J. F. Mitchell, D. N. Argyriou, and L. C. Chapon, *Phys. Rev. B* **70**, 174433 (2004).

²¹I. G. Daec, S. V. Diaz, B. G. Kim, S.-W. Cheong, and P. Schiffer, *Phys. Rev. B* **65**, 174426 (2002).